

H. A. ELLEBY

F. W. KLAIBER

MARCH 1970

ISU-ERI-AMES-69000

PRELIMINARY STUDIES OF REMEDIAL MEASURES FOR THE PREVENTION OF BRIDGE DECK DETERIORATION

PROJECT HR-146
IOWA STATE HIGHWAY COMMISSION
IOWA HIGHWAY RESEARCH BOARD
AMES, IOWA 50010

ERI Project 816-S

TA1
108p
816-S

ENGINEERING RESEARCH INSTITUTE
IOWA STATE UNIVERSITY
AMES, IOWA 50010 USA

**ENGINEERING
RESEARCH**

**ENGINEERING
RESEARCH**

**ENGINEERING
RESEARCH**

**ENGINEERING
RESEARCH**

**ENGINEERING
RESEARCH**

**PRELIMINARY STUDIES OF REMEDIAL
MEASURES FOR THE PREVENTION
OF BRIDGE DECK DETERIORATION**

Dr. H. A. Elleby and Dr. F. W. Klaiber
Co-Principal Investigators

March 1970

Contract HR-146

The opinions, findings, and conclusions expressed in
this publication are those of the authors and not
necessarily those of the Iowa State Highway Commission

*ISU-ERI-AMES-69000
ERI Project 816-S*

**ENGINEERING RESEARCH INSTITUTE
IOWA STATE UNIVERSITY AMES**

1. Report No. ISU-ERI-AMES-69000		2. Government Accession No.		3. Recipient's Catalog No.	
4. Title and Subtitle PRELIMINARY STUDIES OF REMEDIAL MEASURES FOR THE PREVENTION OF BRIDGE DECK DETERIORATION				5. Report Date March 1970	
				6. Performing Organization Code	
7. Author(s) H. A. Elleby and E. W. Klaiber				8. Performing Organization Report No. ISU-ERI-AMES-69000	
9. Performing Organization Name and Address Engineering Research Institute Iowa State University Ames, Iowa 50010				10. Work Unit No.	
				11. Contract or Grant No. HR-146	
12. Sponsoring Agency Name and Address Iowa Highway Research Board Iowa State Highway Commission Ames, Iowa 50010				13. Type of Report and Period Covered	
				14. Sponsoring Agency Code	
15. Supplementary Notes					
16. Abstract <p>Four series of five specimens each were investigated for static and fatigue strength. These four series differed in that there were two variables, the first being the subsidence of concrete around reinforcing bars and the second being shrinkage due to two different curing conditions. The combinations of these variables were then compared to each other by use of load-deflection curves and S-H fatigue curves.</p>					
17. Key Words Bridge Fatigue Concrete Slab Cracking Steel-reinforcement				18. Distribution Statement Unlimited	
19. Security Classif. (of this report) Unclassified		20. Security Classif. (of this page) Unclassified		21. No. of Pages 22	
				22. Price \$3.00	

CONTENTS

	Page
LIST OF FIGURES	ii
LIST OF TABLES	iii
INTRODUCTION	1
TEST PROGRAM	2
Materials	3
Test Procedure	3
Specimen Preparation	3
Equipment and Testing Procedure	5
Test Results	11
SUMMARY AND CONCLUSIONS	14
Deflections of Static Tests	14
Fatigue Tests	18
FUTURE WORK	21
ACKNOWLEDGMENT	22

LIST OF FIGURES

	Page
1. Typical stress-strain curve of longitudinal reinforcement.	3
2. Cross section of typical slab specimen.	4
3. Top bar support for Series III and IV.	5
4. Simulation of field conditions.	10
5. Typical test specimen in fatigue frame.	12
6. Typical end support restraint.	12
7. Center line load deflection curves for Series I.	14
8. Center line load deflection curves for Series II.	14
9. Center line load deflection curves for Series III.	14
10. Center line load deflection curves for Series IV.	14
11. Average center line load deflection curves for Series I - IV.	15
12. Tested specimens of Series I.	16
13. Tested specimens of Series II.	16
14. Tested specimens of Series III.	17
15. Tested specimens of Series IV.	17
16. S-N curves for fatigue specimens, Series I - IV.	18

LIST OF TABLES

	Page
1. Series I Test Data	6
2. Series II Test Data	7
3. Series III Test Data	8
4. Series IV Test Data	9

INTRODUCTION

For many years one of the most frequent and troublesome aspects of bridge maintenance has been the repair of deteriorating bridge decks. This problem exists in all areas of the United States. Therefore, possible remedial measures should be investigated concerning probable causes of the deterioration.

This deterioration may result from chemical and/or mechanical effects such as calcium chloride and freeze-thaw action, which occur mainly in the colder climates of the United States, as well as fatigue loading on the slab.

Another cause of bridge deck deterioration is the interrelationship of fatigue loading on the slab and shrinkage and subsequent destruction of the slab. Shrinkage of the concrete has a two-fold effect. First, if the percentage of reinforcement is high enough, the concrete tends to crack due to induced tensile forces in the concrete created by the resistance of steel to the shrinkage strains. Second, as the concrete cures, the concrete aggregate tends to subside while bleeding occurs. This subsidence is thought by many researchers to weaken the bond on the bottom of the bar and even to cause cracking at this level at the time of set. This latter problem is being studied by Derwin Merrill, staff member of the Civil Engineering Department of Iowa State University.

TEST PROGRAM

The proposed test program was designed to

- determine to what degree the two problems mentioned above contribute to bridge slab deterioration under fatigue loading,
- propose possible remedial measures, and
- determine how well these remedial measures help alleviate these problems.

The test program involved 20 simulated bridge slab sections. Three of every five of these slabs were fatigue tested using repeated loading. By constructing some slabs with normal construction techniques and others with various combinations of remedial methods, it was possible to determine the effects of such remedial measures on fatigue strength.

Results from fatigue tests on standard slab cross sections were compared to fatigue results obtained from slabs constructed with unchaired top bars, slabs cured in dry conditions, and a combination of the two. The unchaired top bars were introduced to eliminate subsidence of the concrete around the bar as a variable acting with the shrinkage of the concrete as another variable. Since this was a pilot program, an absolute minimum number of specimens were cast. To obtain reasonable results, three specimens for the fatigue tests plus two additional specimens for static testing were required. Thus there were five slab sections with standard reinforcing steel supports wet cured, five with standard reinforcing steel supports dry cured, five with unchaired top reinforcing steel wet cured, and five with unchaired top reinforcing steel dry cured. In the fatigue testing of the specimens, the fatigue testing machine was used at a load range sufficient to result in failure in the range of 100 to 1000 kilocycles.

Materials

All specimens were made with a D57 mix made from Type I Portland cement. Proportions by weight were 1:2:2 with 3/4-in. maximum size aggregate. The mix was provided by a local concrete ready-mix plant, and was delivered by truck to the laboratory. All specimens within one series were cast from the same batch of concrete in order to obtain uniformity in material properties of the slabs. For the D57 specifications a minimum 28-day strength of 4050 psi was expected for the specified water cement ratio of 4.63 gal/sack.

The reinforcement consisted of No. 5 deformed bars of Grade 60 for the longitudinal reinforcement and Grade 40 for the transverse reinforcement. Both grades meet the requirements of ASTM A-615. In Fig. 1, a typical stress-strain curve of the longitudinal reinforcement is shown. The average yield point of the longitudinal steel was about 79 ksi, the ultimate strength 114 ksi, and the modulus of elasticity taken to be 29,000 ksi.

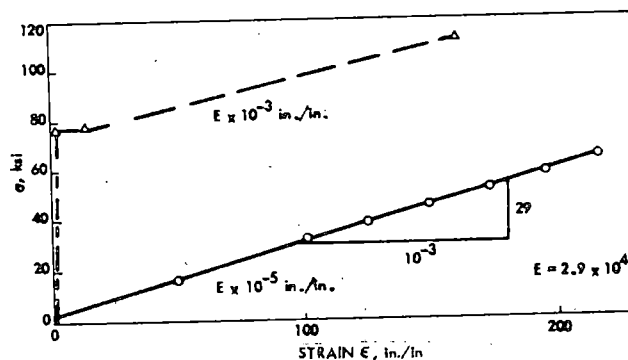


Fig. 1. Typical stress-strain curve of longitudinal reinforcement.

ultimate strength 114 ksi, and the modulus of elasticity taken to be 29,000 ksi.

Test Procedure

Specimen Preparation

The 20 specimens tested were cast in lots of five; thus four pours were necessary for the complete casting. Commercial metal forms were used for specimens. The size of the specimens and location of the reinforcing steel

is shown in Fig. 2. At the pouring of each series of simulated slabs (five specimens), 12 control cylinders were made for determining concrete strength,

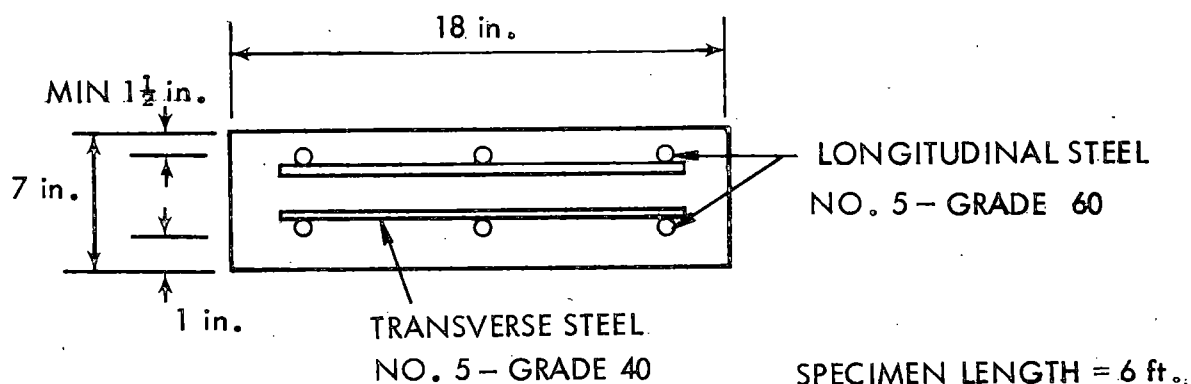


Fig. 2. Cross section of typical slab specimen.

f'_c , at the time of tests. Also, the concrete slump was measured at the start and finish of each pour. The average value of the slump and the concrete strength is reported in Tables 1 - 4. During placement of the concrete, a mechanical vibrator was used to eliminate voids. Two inserts were located in each beam about one foot from each end of the specimens for ease of handling.

After the initial set occurred, all slabs were covered first with wet burlap, then with polyethylene. The beams were kept wet for at least three days, after which each of the series was handled as follows. Series I and II were cast using standard chairs for supporting the bars. Series I was cured under conditions approaching 100% relative humidity from casting to testing, while Series II was kept wet only for the first three days; then cured in air until time of testing.

Series III and IV were cast using the standard slab bolsters (SB) for supporting the bottom bars only. The top bars were supported by wires as shown in Fig. 3.

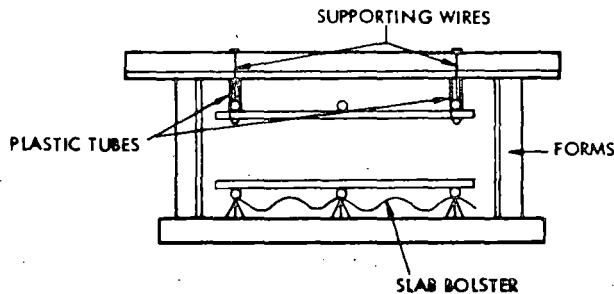


Fig. 3. Top bar support for Series III and IV.

Four wires were used for each specimen to support the top transverse bars. These wires were adjusted so the initial position of the top bars was the same as that of the top bars in Series I and II. After the placement, vibration, and initial screeding of the concrete in the form, the wires were cut to permit the top reinforcement to settle as the concrete subsided. These wires were placed in plastic tubes (Fig. 3), thus eliminating friction between the concrete and wire. After initial curing, Series III was air dried while Series IV was cured similarly to Series I.

Equipment and Testing Procedure

All specimens were inverted before testing. Thus, what was the bottom steel when cast became the top steel, and the top steel during casting became the bottom steel. This inversion of the specimen was easily accomplished by using a set of plywood wheels which slipped over each end of the slab. The specimens were then simply "rolled-over." This inversion simulated the slab in the negative moment region over the piers (see Fig. 4a). The length of the model simulation shown in Fig. 4b is such that the supports occur at about the location of the inflection points. The exact location of the inflection point depends on the loading and span length (distance between piers) in question. This laboratory model then simulates the condition of zero moment at the

Table 1. Series I Test Data.

(A) Deflection from static tests.

Slump = 3.88 in.

Deflections					
Specimen 1			Specimen 2		Average
Load (kips)	ϵ (in. $\times 10^{-3}$)	$\frac{1}{4}$ pt (in. $\times 10^{-3}$)	ϵ (in. $\times 10^{-3}$)	$\frac{1}{4}$ pt (in. $\times 10^{-3}$)	ϵ (in. $\times 10^{-3}$)
0	0	0	0	0	0
0.5	6.5	5.0	5	2	6.5
1	9.0	6.5	8	4	7
2	17.0	11.5	15	6	12.5
3	26.5	16.5	18	11	20.8
4	38.0	23.5	30	18	28
5	48.5	30.0	43	25	39.3
6	59.5	36.5	61	37	51.3
7	69.5	42.5	80	50	65.3
8	79.5	49.5	100	62	79.8
9	91.0	56.0	118	73	95.5
10	104.5	63.5	134	84	111.3
11	119.0	73.0	150	93	126.5
12	136.5	83.5	171.5	106.5	143.3
13	154.0	94.0	189.5	119.5	162.8
14	171.5	104.5	209	132	180.5
15	199.0	127.0	228	145	204
16	225.0	145.0	247	157	226.5
17	244.0	158.0	265	170	245.5
18	267.0	169.0	284	184	266
19	292.0	196.0	306.5	197.5	288
20	318.0	214.0	334.5	214.5	312.3

(B) Static test final results, average failure load = 23.25k.

	Specimen 1	Specimen 2
Failure load (kips)	22.5	24.0
Type failure	Shear-Bond	Flexure
Age (days)	38	43
f'_c , average (psi)	3243	3940

(C) Fatigue test results.

	Specimen 3	Specimen 4	Specimen 5
Load (kips)	15.75	13.5	11.25
% of ultimate	70	60	50
Calculated max. stress (ksi)	62.5	53.7	44.7
No. cycles	77,010	199,150	636,150
Age (days)	51	57	63
f'_c , average (psi)	4111	4308	4294

Table 2. Series II Test Data.

(A) Deflection from static tests.

Slump = 3.50 in.

Load (kips)	Deflections				
	Specimen 1		Specimen 2		Average
	ϵ (in. $\times 10^{-3}$)	$\frac{1}{4}$ pt (in. $\times 10^{-3}$)	ϵ (in. $\times 10^{-3}$)	$\frac{1}{4}$ pt (in. $\times 10^{-3}$)	ϵ (in. $\times 10^{-3}$)
0	0	0	0	0	0
0.5	3	2	2.5	4	2.75
1	5.5	4	5.5	5.5	5.5
2	11.0	7.5	10.0	9.0	10.5
3	19.5	12.5	14.5	12.0	17.0
4	31.0	19	25.0	19.0	28.0
5	50.5	30.5	46.0	31	48.3
6	70.0	41.5	65.0	42.5	67.3
7	95.0	56.5	87.5	55.0	91.3
8	114.0	69.0	106.5	67.5	111.5
9	138.5	83.0	126.0	80.0	133.8
10	157.5	96.2	147.5	92.0	152.5
11	177.0	110.0	165.0	104.0	171.0
12	198.5	124.0	183.5	116.0	191.0
13	221.0	140.0	202.5	129.0	211.8
14	243.0	154.5	221.0	141.0	232.0
15	266.5	169.0	242.0	154.0	254.3
16	290.0	184.5	262.5	167.0	276.3
17	310.5	197.5	281.5	178.5	296.0
18	333.0	212.0	300.0	191.0	316.5
19	356.0	227.0	320.5	203.0	338.3
20	—	—	—	—	—

(B) State test final results, average failure load = 25.50k.

	Specimen 1	Specimen 2
Failure load (kips)	24.7	26.3
Type Failure	Flexure	Flexure
Age (days)	54	56
f'_c average (psi)	4364	4341

(C) Fatigue test results.

	Specimen 3	Specimen 4	Specimen 5
Load (kips)	12.98	15.57	10.34
% of ultimate	50	60	40
Calculated max. stress (ksi)	51.7	62.0	41.2
No. cycles	270,440	110,490	422,450
Age (days)	62	62	—
f'_c , average (psi)	4504	4504	4504

Table 3. Series III Test Data.

(A) Deflection from static tests.

Slump = 2.00 in.

Deflections

Load (kips)	Specimen 1		Specimen 2		Average
	ϵ (in. $\times 10^{-3}$)	$\frac{1}{4}$ pt (in. $\times 10^{-3}$)	ϵ (in. $\times 10^{-3}$)	$\frac{1}{4}$ pt (in. $\times 10^{-3}$)	ϵ (in. $\times 10^{-3}$)
0	0	0	0	0	0
0.5	3	0	4.5	4	3.75
1	5	0	7.5	7	6.25
2	12.5	0	14.5	12	13.5
3	19	0	21	18	20
4	37	12	34.5	26	35.75
5	56	25	48.5	37	52.25
6	91	47	76	55	83.5
7	118.5	68	97.5	70	108
8	140	80	119	85	129.5
9	164.5	95	138	98	151.25
10	189	110	156.5	110	172.75
11	209	129	178	125	193.5
12	231.5	144	197	139	214.25
13	257.5	160	218	153	237.75
14	277.5	173	239	167	258.25
15	301	189	263	182	282
16	327.5	210	285	197	306.25
17	350.5	225	305	213	327.75
18	378	246	325.5	227	351.75
19	—	—	347	241	—
20	—	—	391.5	268	—

(B) Static test final results, average failure load = 24.35k.

	Specimen 1	Specimen 2
Failure load (kips)	23.7	25.0
Type failure	Flexure	Flexure
Age (days)	62	62
f'_c , average (psi)	5464	5464

(C) Fatigue test results.

	Specimen 3	Specimen 4	Specimen 5
Load (kips)	14.61	10.24	12.18
% of ultimate	60	40	50
Calculated max. stress (ksi)	57.5	40.4	48.3
No. cycles	125,880	880,050	223,340
Age (days)	65	74	81
f'_c , average (psi)	5500	5853	5616

Table 4. Series IV Test Data.

(A) Deflection from static test.

Slump = 2.00 in.

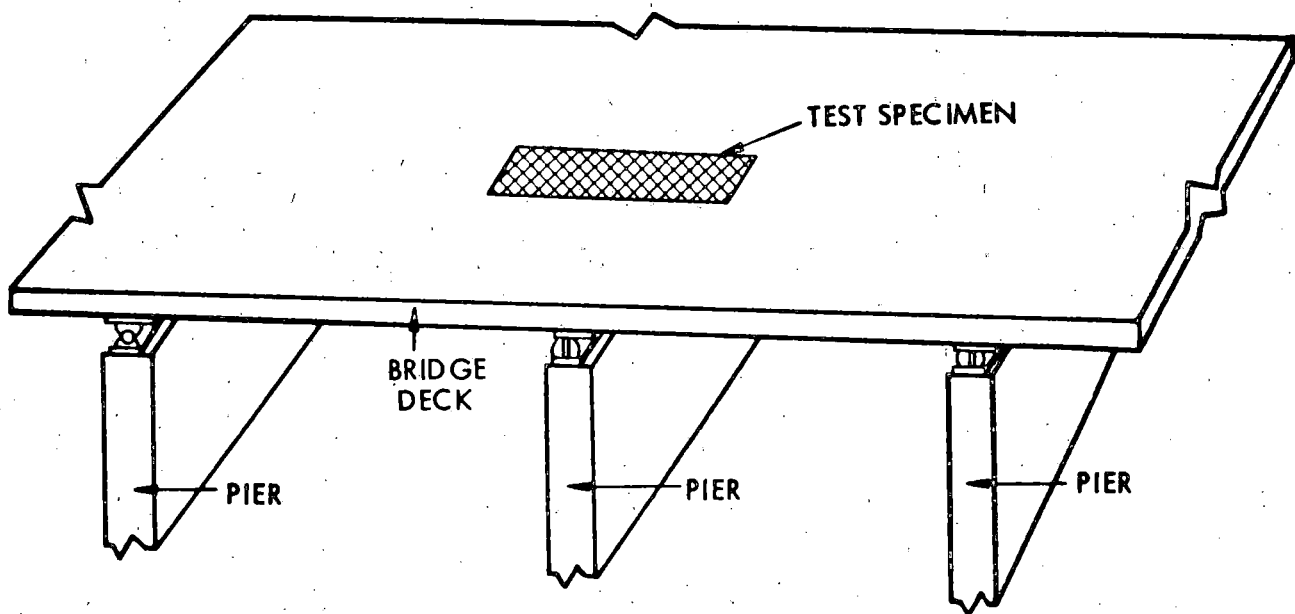
Deflections					
Load (kips)	Specimen 1		Specimen 2		Average
	ϵ (in. $\times 10^{-3}$)	$\frac{1}{4}$ pt (in. $\times 10^{-3}$)	ϵ (in. $\times 10^{-3}$)	$\frac{1}{4}$ pt (in. $\times 10^{-3}$)	ϵ (in. $\times 10^{-3}$)
0	0	0	0	0	0
0.5	4	5	4	3.5	4
1	7	9	6.5	6.5	6.75
2	13	14	12	11.5	12.50
3	18	20	19	17	18.50
4	22.5	24	28	24	25.25
5	27	28	44.5	36	35.75
6	36	35	61.5	48	48.75
7	56	49	80.5	62	68.25
8	80	64	97.5	74	88.75
9	101	79	118.5	87	110.75
10	119	91	136	98.5	127.50
11	140	104	153.5	111	146.75
12	156.5	115	172	123	164.25
13	180.5	131	190	137	185.25
14	199	144	208.5	150	203.75
15	216	155	229.5	164	222.75
16	240	176	250	178	245
17	259	189	269.5	191	264.25
18	277	201	288.5	204	283.75
19	298.5	214	310	219	304.25
20	322.5	230	352.5	—	337.50

(B) Static test final results, average failure load = 25.45k.

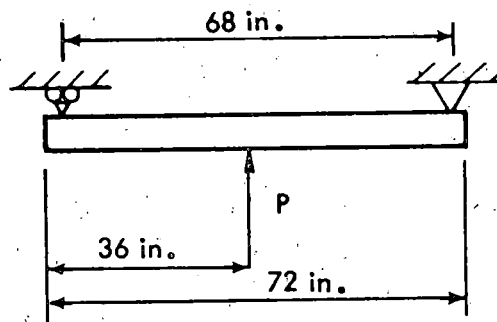
	Specimen 1	Specimen 2
Failure load (kips)	25.9	25.0
Type failure	Shear-Bond	Flexure
Age (days)	70	76
f'_c , average (psi)	5800	5871

(C) Fatigue test results.

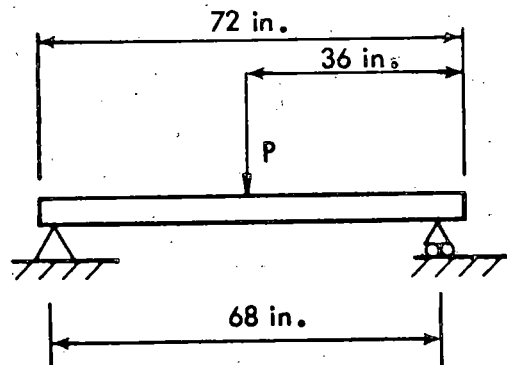
	Specimen 3	Specimen 4	Specimen 5
Load (kips)	12.75	15.77	10.00
% of ultimate	50	62	39.3
Calculated max. stress (ksi)	50.1	62.2	39.3
No. cycles	148,040	63,380	532,370
Age (days)	79	81	111
f'_c , average (psi)	5990	5950	6720



(a) Location of test specimen with respect to prototype bridge.



(b) Model simulation.



(c) Laboratory simulation.

Fig. 4. Simulation of field conditions.

inflection points, but the deflection at the support points is zero which obviously is not the case in the field. However, the relative differential settlement is closely approximated.

Two specimens of each series were static tested in a 400^k Baldwin compression testing machine. Deflections at both the center line and 1/4 points were measured during the static tests.

Fatigue tests were performed on the remaining 12 beams (three from each series). The fatigue tests were conducted in a self-contained frame employing MTS closed-loop fatigue equipment. This equipment applied a sinusoidal loading at the center line of the 68-in. simple span at the rate of 1.2 cps. Figure 5 shows a specimen in the fatigue testing frame. A close-up of the restraint to the roller and pin supports of the specimen is shown in Fig. 6. This restraint was required to keep the specimen from vibrating off the supports.

The fatigue equipment compared the desired input load with the actual applied load and when a 10% difference was sensed, the test was automatically shut off. When the specimen failed, the machine was automatically shut off by a circuit breaker triggered by a cord being pulled by the broken beam.

Test Results

The load-deformation data for the two static tests from each of the four series of test specimens are shown in Tables 1(A) - 4(A). These tables also show the average center-line deflection for each of the two tests in each series.

The ultimate static load, type of failure, age of specimen, and 28-day cylinder strength for the static tests from Series I - IV is shown in Tables 1(B) - 4(B) respectively.

The data from the fatigue tests conducted on three specimens from each series is shown in Tables 1(C) - 4(C). These tables list the maximum load

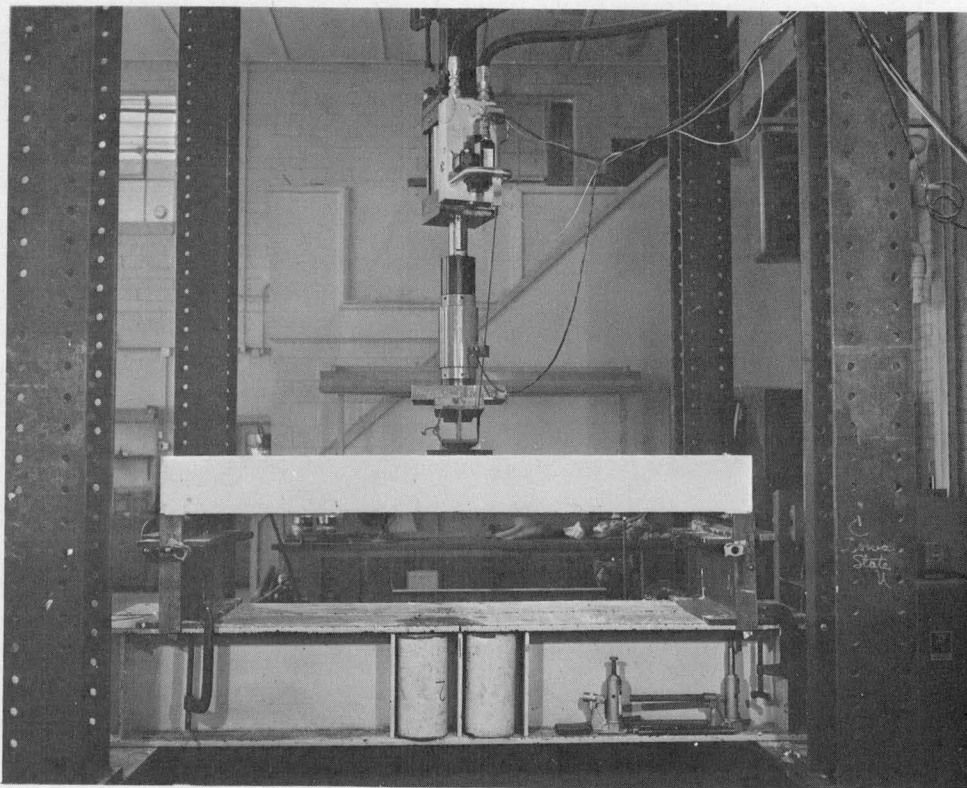


Fig. 5. Typical test specimen in fatigue frame.

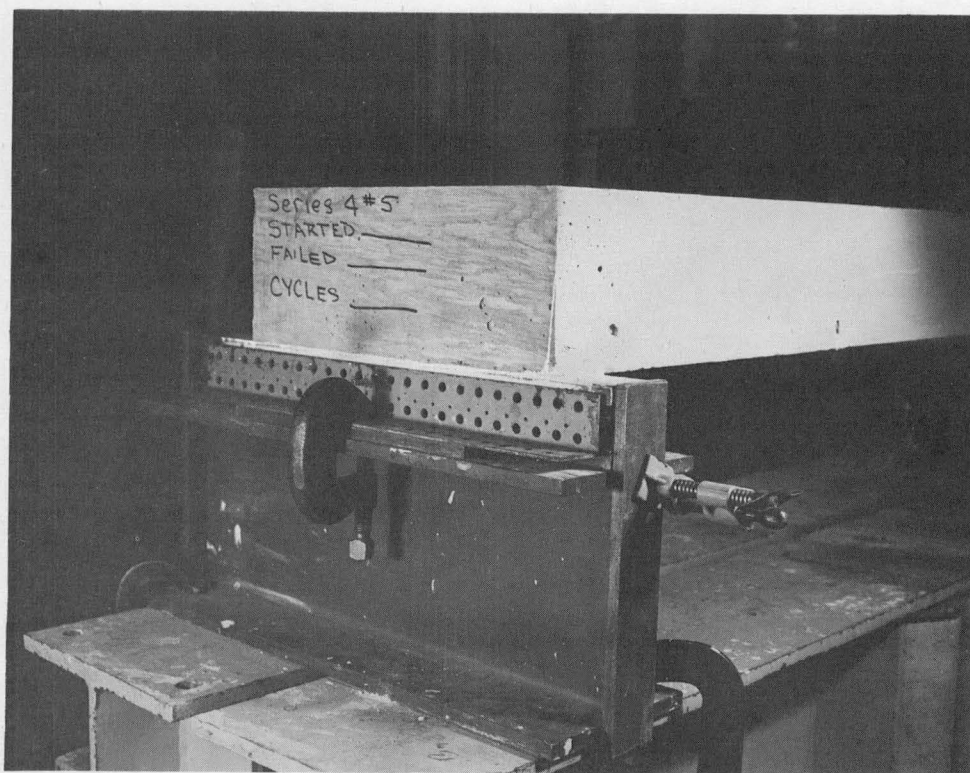


Fig. 6. Typical end support restraint.

percent of ultimate static load, maximum steel stress, the number of cycles to failure, ages of specimens upon failure, and the average 28-day cylinder strength. The minimum load on all fatigue tests was a constant value of 0.5^k which was used to prevent excessive walking of the specimen.

SUMMARY AND CONCLUSIONS

Deflections of Static Tests

The static test data reported in Tables 1(A) - 4(A) for the deflection of each test in each series are plotted in Figs. 7 - 10. In each of these figures, the center-line deflection of each of the two tests in a single series is plotted. As may be noted, the differences in deflection at various load levels is of an acceptable magnitude. Figure 11 shows the average center-line deflection of the two specimens in each series. It can be seen that the specimens that were moist cured up to time of test (Series I and IV) display a greater stiffness

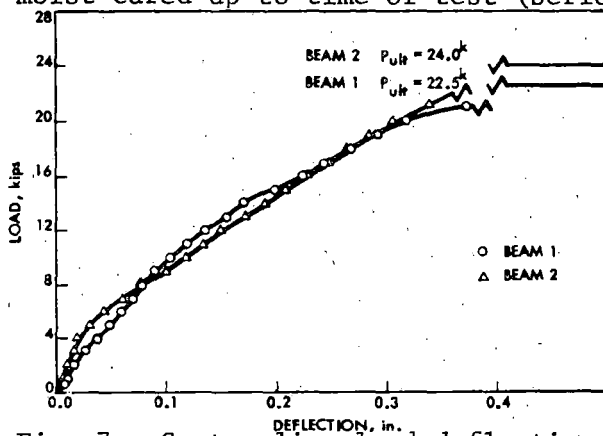


Fig. 7. Center-line load deflection curves for Series I.

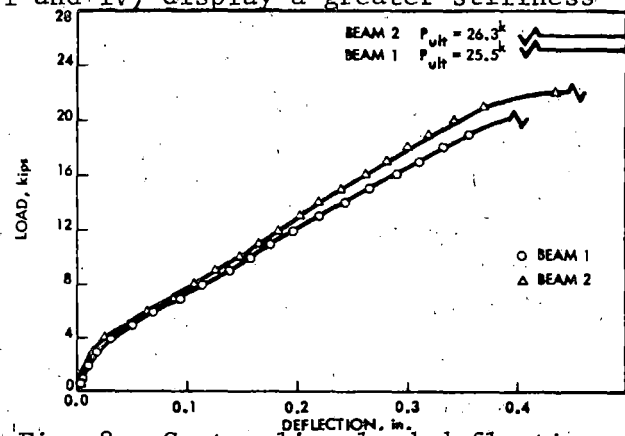


Fig. 8. Center-line load deflection curves for Series II.

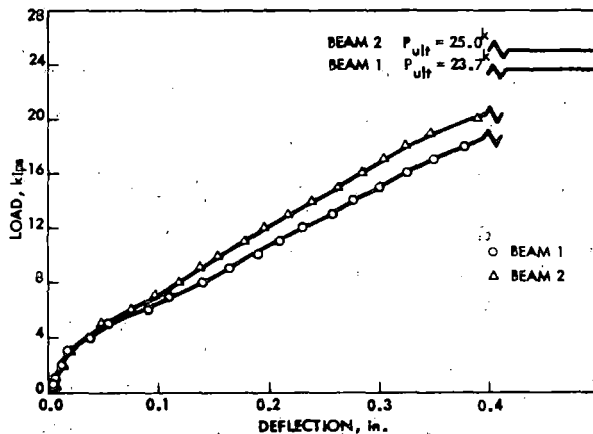


Fig. 9. Center-line load deflection curves for Series III.

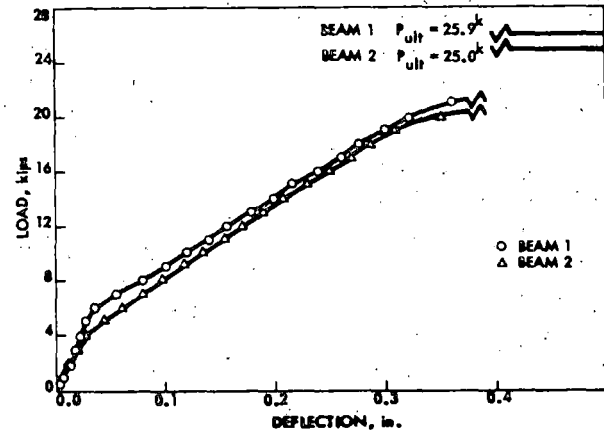


Fig. 10. Center-line load deflection curves for Series IV.

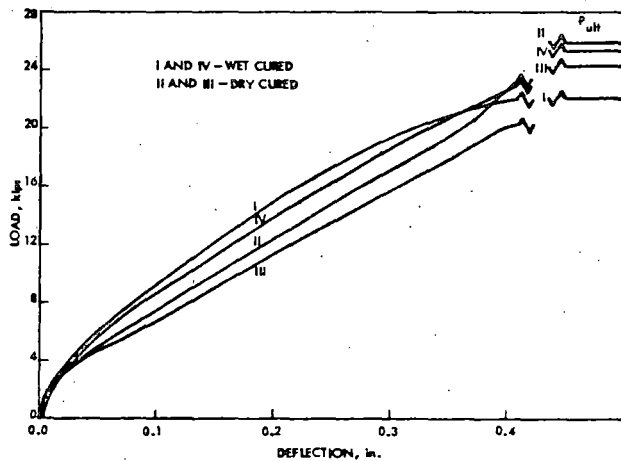


Fig. 11. Average center-line load deflection curves for Series I - IV.

This type of failure was also noted in static test No. 1 of Series IV, as may be seen in Fig. 15. These failures were caused because both series were kept wet until the time of the first static test. It is well known that the wetness of concrete will affect tension strength to a greater extent than compression strength, thus forcing the failure of the specimen from a ductile-flexure failure to a shear-bond failure.

As can be seen in the photographs of Series II and III (Figs. 13 and 14), all failures of the static tests (Nos. 1 and 2 of each series) were flexure failures except as noted above.

From the available data, it seems evident that the load deflection relationship is more dependent on the curing condition of the specimens than on elimination of possible subsidence cracks around the reinforcement.

It can also be seen from Fig. 11 that the ultimate strength of the members varies from an average value of only plus or minus 10%. This is expected since the ultimate moment capacity is essentially independent of

than the beams cured in air (Series II and III). This is most likely caused by the greater shrinkage stresses in the air dried specimens. This can also be seen in the difference in cracking load of each of the four series shown in this figure. The first static test of Series I displayed a shear-bond failure which can be seen in Fig. 12.

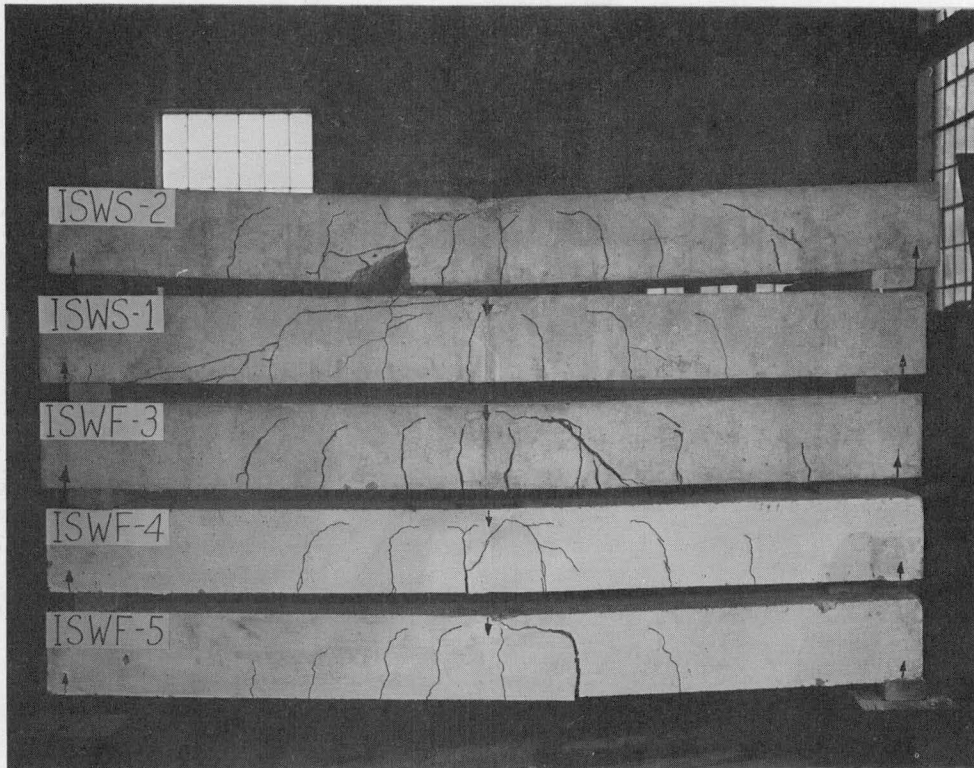


Fig. 12. Tested specimens of Series I.

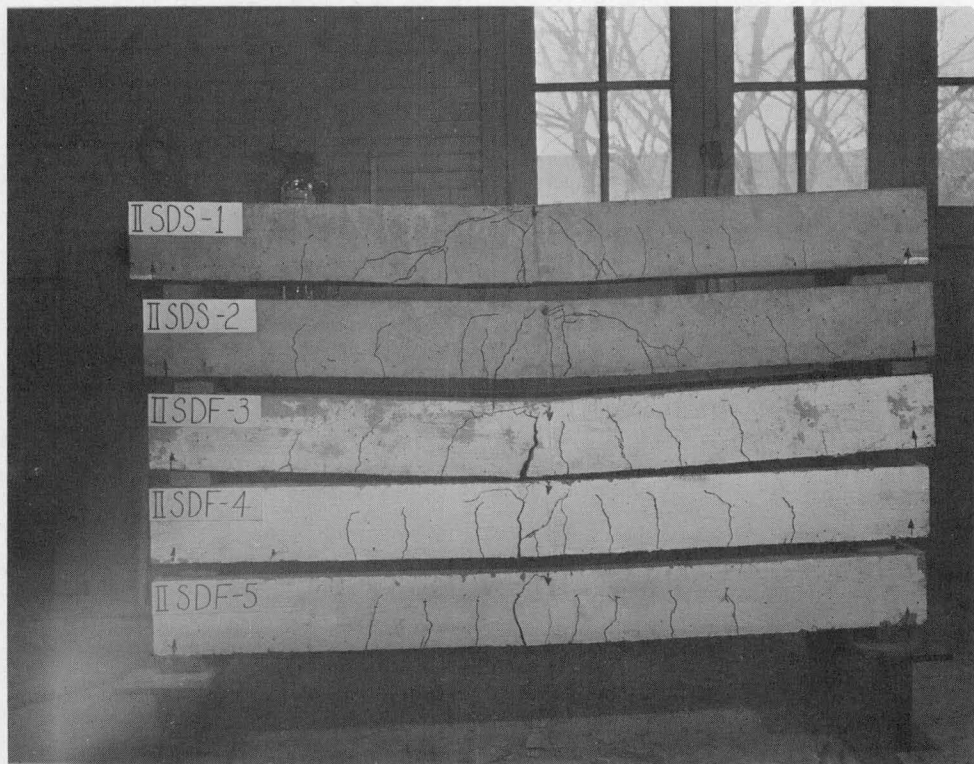


Fig. 13. Tested specimens of Series II.

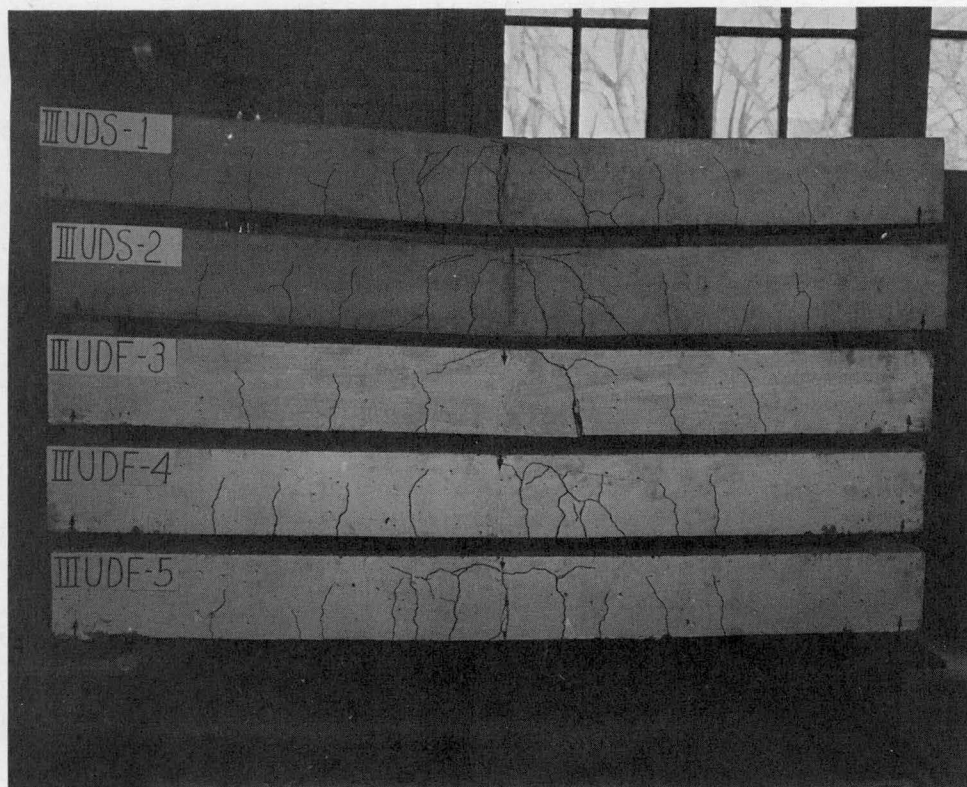


Fig. 14. Tested specimens of Series III.



Fig. 15. Tested specimens of Series IV.

concrete strength for a given beam geometry and steel percentage. Note that the ultimate strength values are not ordered in the same sequence as the initial portions of the load deflection curves.

Fatigue Tests

The data reported in Tables 1(C) - 4(C) are plotted in Fig. 16, which shows the normal stress-strain log-log curve used in reporting data from fatigue tests. A regression line analysis was run on this data including all

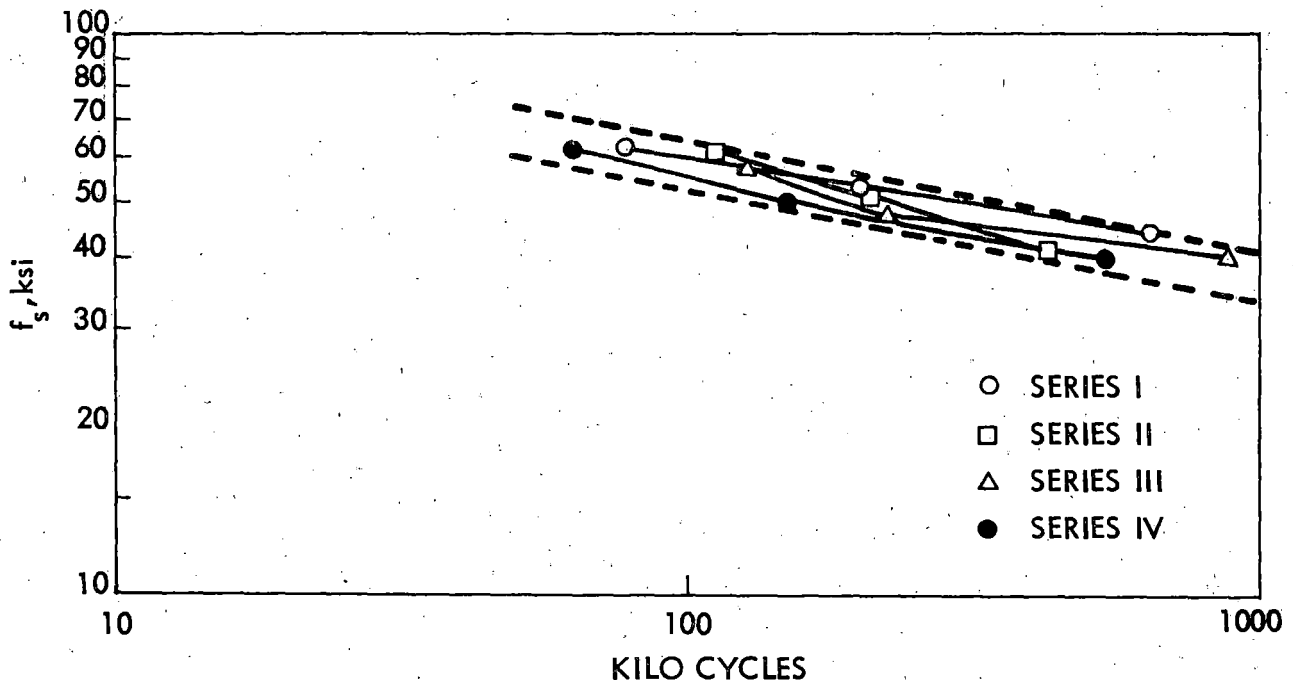


Fig. 16. S-N curves for fatigue specimens, Series I - IV.

points. The resulting equation is

$$f_s = 4.945e^{-.19N},$$

where f_s is the stress (ksi), and N is the number of kilocycles. The coefficient of correlation for the test data was 0.94 where 1.00 would be perfect correlation.

This equation is plotted on Fig. 16 as two lines deviating from the

actual equations by plus or minus 10%. It can be seen that all the data falls within this band indicating a low level of significance for the differences between the various series. From Figs. 12 - 15, it can be seen that the fatigue failures (Nos. 3 - 5 of each series) were flexural failures, in most of which bar breakage occurred.

The occurrence of bar breakage for low percentage reinforcement has been found to be common by numerous other researchers. An example is the work done by the Portland Cement Association.

In the majority of these tests, there is little evidence of concrete deterioration in the compression zone. However, numerous cracks were present in the tension zone, which can be seen in the photographs of Figs. 12 - 15.

This tension zone was considerably weakened by this cracking and frequently loose material would drop from the cracks during fatigue testing. This seems to indicate that with truck traffic and extensive cracking, gradual mechanical deterioration of the concrete could occur if the steel stresses were held below the endurance limit.

In conclusion, since there were no significant differences in fatigue strength of the four series as indicated in the S-N curve of Fig. 16, it can be stated that the curing conditions influence the load deflection characteristics although they do not influence the fatigue characteristics. This can also be said about the effect of concrete subsidence around the reinforcing steel. Since there seemed to be such little influence of subsidence on fatigue or static strength, it was not felt that it was necessary to core these slabs to measure actual displacement of the "freely" supported reinforcing bars.

This does not mean that the variables investigated in this program would be of no importance to bridge deterioration in the long run. For example, dry curing will not appreciably affect ultimate strength, but will lead to excessive

cracking, which in turn permits easy entrance of deicing salts and other corrosive and deleterious substances to the reinforcing steel. This, in turn, will lead to spalling of the concrete as has been shown in other research in this area.

FUTURE WORK

From the preliminary test program, it was found that deterioration in the bridge deck can not be attributed to short-time effects except for cracking in the tension zones. To further explore the problem of bridge deck deterioration, we must look to the long-term effects of shrinkage and subsidence.

One problem would be to determine whether cracks in the bridge slab which become filled with debris as a result of fatigue stress in the concrete or other sources would reduce the stress range through which the tension steel is worked during live load application. This would greatly increase the fatigue life of the steel while causing stress concentrations in the concrete, which may lead to possible deleterious effects resulting in failure.

At present the long-term effects of deicing chemicals is being investigated by others.

ACKNOWLEDGMENT

This research was conducted by the Structural Engineering Research Laboratory staff, Engineering Research Institute, Iowa State University, Ames, and was sponsored by the Iowa State Highway Commission.

The authors appreciate the assistance of Dr. Carl E. Ekberg, Head, Department of Civil Engineering, who was available as a special consultant.

The assistance and cooperation of many persons in making suggestions and furnishing information on the conduct of this study is acknowledged.